On-resonance angular distributions were placed on an absolute cross-section scale with these excitation functions. Absolute differential cross sections are assigned a $\pm 25\,\%$ uncertainty whereas angular distribution data were ordinarily reproducible to within $\pm 3\,\%$. The α-beam energy was calibrated with the $^{7}Li(\alpha, n)^{10}B$ reaction having a threshold at $E_\alpha = 4.3843$ MeV.

4. Elastic scattering of α-particles from ^{29}Si

Excitation functions for $^{29}Si(\alpha, \alpha)^{29}Si$ measured in energy steps of 250 keV at angles from 50° to 165° in 15° steps are presented in figs. 1 and 2. Angular distributions also measured at 3.0, 4.5 and 5.5 MeV in angular steps of 5° are shown in fig. 3. The code ABACUS [10]) was used in conjunction with the Woods-Saxon volume absorption potential,

$$V = 190 \text{ MeV}, \quad W_v = 10 \text{ MeV},$$

$$R = R_v = 1.176(4^{\frac{1}{3}} + A^{\frac{1}{3}}) \text{ fm},$$

$$a = a_v = 0.576 \text{ fm},$$

to calculate elastic cross sections. This potential proved consistent with the four $(\alpha, \mathcal{N})$ reactions and elastic scattering from ^{13}C, ^{19}F, ^{29}Si and ^{31}P targets with the exception that the imaginary potential was reduced to 6 MeV in the ^{13}C case. These calculated cross sections for ^{29}Si, plotted as solid curves in figs. 1–3, display agreement on the average with the experimental data.

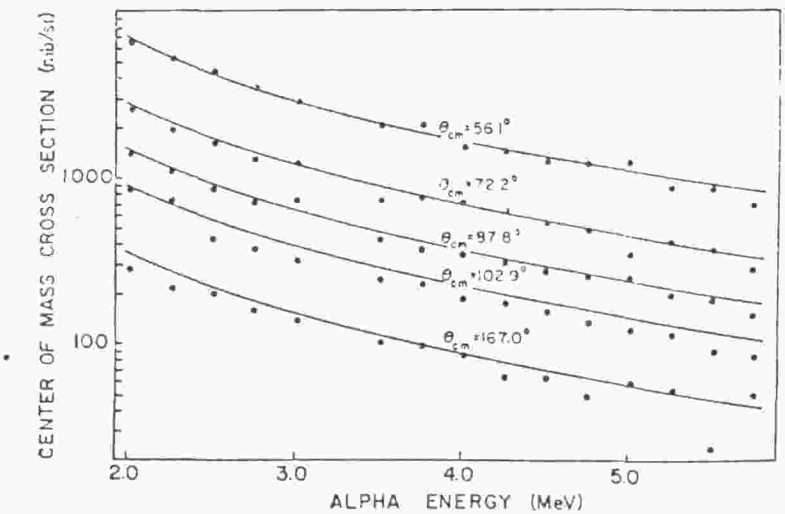

Fig. 1. Excitation functions measured for $^{29}Si(\alpha, \alpha)^{29}Si$ at 56.1, 72.2, 87.8, 102.9 and 167.0° c.m. angles. The curves are calculated with the code ABACUS incorporating a volume absorption Woods-Saxon type potential $V = 190$ MeV, $W_v = 10$ MeV, $R = R_v = 1.176(4^{\frac{1}{3}} + A^{\frac{1}{3}})$ fm and $a = a_v = 0.576$ fm.

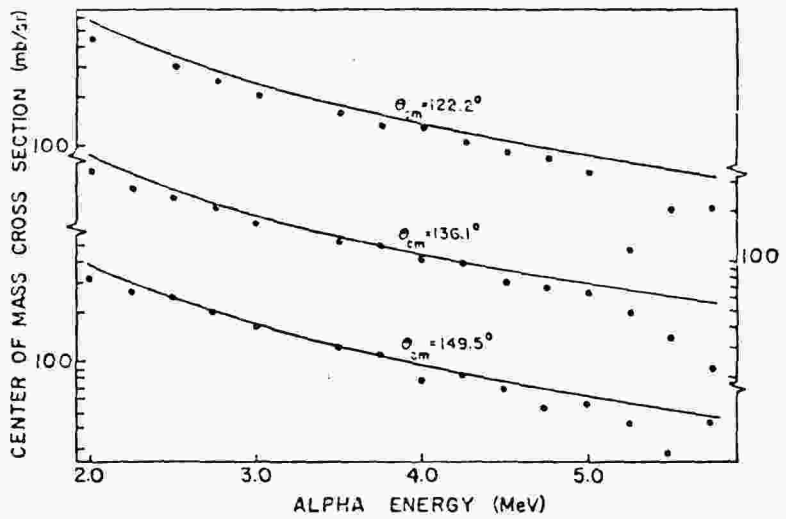

Fig. 2. As fig. 1, but at 122.2, 136.1 and 149.5° c.m. angles. The right hand scale pertains to the intermediate excitation function.

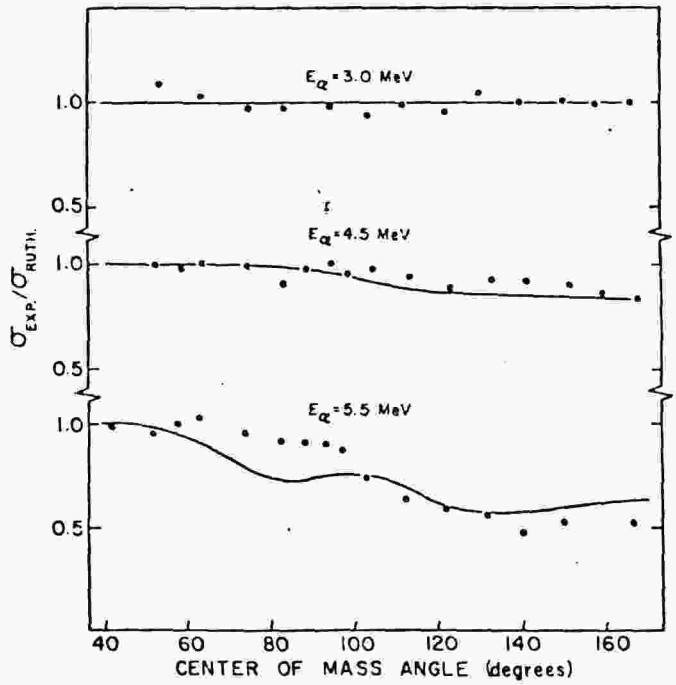

Fig. 3. Angular distributions of measured-to-Rutherford cross-section ratios for the $^{29}Si(\alpha, \alpha)^{29}Si$ reaction. The curves are calculated as in fig. 1.

TABLE 1

Transmission coefficients, T_l, calculated with code ABACUS for α-particles on ^{29}Si at representative energies, E_x

T_l	E_α (MeV)							
	3.675	3.875	4.135	4.325	4.635	4.975	5.235	5.410
T_0	0.0686	0.1118	0.1869	0.2517	0.3639	0.4796	0.5556	0.5998
T_1	0.0291	0.0512	0.0967	0.1439	0.2459	0.3832	0.4932	0.5643
T_2	0.0257	0.0455	0.0854	0.1258	0.2096	0.3167	0.3995	0.4524
T_3	0.00510	0.00973	0.0206	0.0338	0.0688	0.1328	0.2024	0.2588
T_4	0.00232	0.00461	0.0101	0.0171	0.0359	0.0712	0.1103	0.1425
T_5	0.000227	0.000474	0.00113	0.00203	0.00485	0.0113	0.0204	0.0294
T_6	0.000054	0.000120	0.000306	0.000571	0.00143	0.00352	0.00651	0.00952
T_7	0.000003	0.000007	0.000019	0.000036	0.000099	0.000269	0.000542	0.000935

Care was taken in establishing this potential to see that the transmission coefficients were smooth functions of energy and angular momentum. Representative transmission coefficients calculated by code ABACUS are presented in table 1.

5. The ^{29}Si(α, n_0)^{32}S excitation functions and normalization procedure

The 0° and 160° excitation functions for the ^{29}Si(α, n_0)^{32}S reaction corrected for neutron background and detection efficiency are shown in fig. 4. On 42 of these resonances, angular distributions were then measured. Initially we concern ourselves only with those angular distributions that are associated with the excitation of a single state in the compound nucleus. Their spin values are readily identified from the unique shapes displayed by these distributions [11]). Unfortunately only seven resonances fall in this single-level category. Therefore, five mixed-level resonances where one of the two states is readily identified as the major cross-section contributor were also selected. These $\theta = 160°$ on-resonance cross sections converted to the c.m. system are plotted versus α-energy in fig. 5 as open symbols.

Differential cross sections calculated and normalized by code MIA are also displayed in fig. 5 as a function of energy and J^π. The single normalization factor of 1.333 multiplying the calculated cross sections brings the curves into approximate agreement with the measured values. Note the order of magnitude cross-section sensitivity to parity for $J \geqq \frac{5}{2}$.

Preliminary to this calculation the transmission coefficients for the competing neutron and proton channels were calculated by means of the computer code SCAT [ref. [12])] using the Wilmore-Hodgson potential [13]) modified to include a spin-orbit potential of 7.5 MeV and the Perey potential [14]) respectively. The α-particle transmission coefficients were discussed earlier.

These transmission coefficients were calculated for the significant channels given in fig. 6 and formed the input to program MANDYF [15]) in which the penetrability factors were calculated. Typical values of these ^{29}Si(α, n_0)^{32}S penetrability factors